ESOMAT 2009, 06013 (2009)
DOI:10.1051/esomat/200906013

Giant elasticity in the Ni-Mn-Ga single crystalline FSMA martensites

I. Glavatskyy[a,1,2], N. Glavatska[1]

[1]Institute for Metal Physics, 36 Vernadsky blvd., Kiev 03142, Ukraine
[2]Helmhotz Centre Berlin for Materials and Energy, Glienicker Str. 100, Berlin 14109, Germany

Abstract. The phenomenon of the giant elastic completely reversible linear strain is found at constant temperatures in Ni-Mn-Ga martensites. Single crystals of some off-stoichiometric Ni-Mn-Ga compositions possess rubber-like behavior in the martensite phase with completely elastic strain reaching over 10% at some 90MPa compressive stress at room temperature. The observed phenomenon is different from the conventional (two-phase) superelasticity, since it is found completely in the martensite phase and no intermartensitic reaction is observed during the load-unload cycling. The main features of the observed rubber-like behavior are: 1) complete elasticity and giant values of the strains achieved; 2) the linear character of stress-strain dependence; 3) excellent stability to the mechanical cycling, stress rate and temperature variation, in contrast to the conventional two-phase superelasticity due to the stress induced martensite transformation. Current work is directed to study the structural mechanisms of the found phenomenon by means of the neutron diffraction in-situ under compressive stress cycling.

1. Introduction

Ni-Mn-Ga alloys are well-known shape memory systems possessing thermoelastic martensitic transformation. Moreover, Ni-Mn-Ga possesses ferromagnetic ordering in martensite phase [1], thus being unique magnetic shape memory alloy (MSMA) system. Mechanical and magnetic properties of Ni-Mn-Ga alloys have been extensively studied. It was shown [2-4] that this alloy system possesses a high pseudoelastic, also called superelastic effect. However, all previously studied stress–strain loops showing pseudoelastic behaviour in these alloys, as well as in most SMA systems such as Ti-Pd-Ni [5], Ni-Ti [6,7], Fe-Pt [8], Cu-Al-X where X is Mn, Zn, Ni [9,10] *etc*. are due to the stress induced martensite transformation (i.e. two-phase superelasticity), and thus, could be obtained only at temperatures above martensite transformation (M_S). This relevantly limits possible technical applications, since most of the systems possessing a pseudoelastic behaviour have M_S above room temperature. The conventional two-phase superelasticity in crystalline SMA possesses several major drawbacks, i.e.: highly nonlinear hysteretic behaviour, strongly dependent on the stress or deformation rates [12,13], not stable with stress cycling, and with strong temperature dependence of the superelastic loop and critical stress values [4,10,11]. While the Ti-Ni [6] seems attractive having 100% recovery and a quasilinear behaviour, though it possesses small elastic strain values (4%) at very high stress values – above 1GPa. On the other hand, in the 20% compressive strain in the martensite phase of single crystalline Ni-Mn-Ga alloy was obtained [14]. However, the crystal faulted, thus strain in the case is not recoverable. Authors [14] obtained 8% shape-memory effect by heating above 400^0C.

We have recently observed and propose another type of superelasticity – completely in the martensite phase of the Ni-Mn-Ga alloys, thus being not temperature sensitive and quasilinear, at the same time reaching high elastic strain values with 100% recovery and stable to cycling.

2. Experimental procedure

Two Ni-Mn-Ga alloys of non-stoichiometric compositions (Table 1) having two main different martensite lattice types were investigated. Single crystals were grown by vertical gradient freeze technique from polycrystalline ingots, initially arc-smelt from 99.98% pure Ni, Mn and Ga chips, which were 4-times sequentially remelted to achieve better chemical homogeneity. Obtained single crystals were heat treated for annealing for homogenization at 1273 K for 72 hours and ordering at 1070 K during 48 hours. All melting and heat treatment

[a] e-mail: illya.glavatskyy@helmholtz-berlin.de

Article available at http://www.esomat.org or http://dx.doi.org/10.1051/esomat/200906013

procedures were carried out under in protective argon with 2%H2 atmosphere. The crystal structure of the martensite phases was determined using X-ray powder diffraction (Fig.1), and orientation of the single crystal specimens was determined using a 3-circle X-Ray diffractometer with the monochromatic CuKα radiation. Temperatures of direct (M_S) and reverse (A_S) martensite transformation and Curie point (T_C) were determined using two standard methods: low field ac-magnetic susceptibility measurements and dilatometry (curves not shown due to limitation of the pictures number). Chemical composition, phase transformation temperatures and martensite lattice parameters are given in Table 1. For simplicity reasons we use fct martensite lattice approximation and indexing system of parent austenite phase. Single crystalline specimens were cut parallel to {100} martensite planes and electropolished in the 25% HNO3 + 75% alcohol electrolyte. Loading speed in the experiments was 0.1-5 mm/min (deformation rate: (R ~ $1*10^{-4}$ up to $8.3*10^{-3}$ s^{-1})). Compressive stress-strain studies were performed by using Tinius-Olsen H1K-T mechanical testing machine with specially constructed narrow blow hot air system for temperature control (δT = ±2K).

3. Results and discussion

All studied alloys possess a thermoelastic martensitic transformation, exhibiting self-accommodation twinned martensite morphology. Alloys 1 has 10M superstructural martensite lattice packing modulation along $<110>_{fct}$ direction [15]. The martensite phase of all alloys has a strong magnetic anisotropy in the ferromagnetic state below T_C, i.e. for alloy 1: $[001]_{fct}$ - axis of easy magnetization, and $[010]_{fct}$ – hard magnetization axis; for alloy 2: $(001)_{fct}$ – easy magnetization plane, with $[001]_{fct}$ being axis of hard magnetization.

Table 1. Compositions, phase transformation temperatures and lattice parameters in ***fct*** martensite approximation according to the parent austenite phase.

alloy	Composition	T_c, K	M_s, K	A_s, K	a, nm *	c, nm *	modulation	distortion
1	$Ni_{1.95}M_{1.20}Ga_{0.85}$	375	307	315	0.593	0.559	10M, $<010>_{fct}$	6%
2	$Ni_{2.13}Mn_{0.78}Ga_{1.09}$	365	465	468	0.540	0.665	none	23%

* *lattice parameters are given for T=293K.*

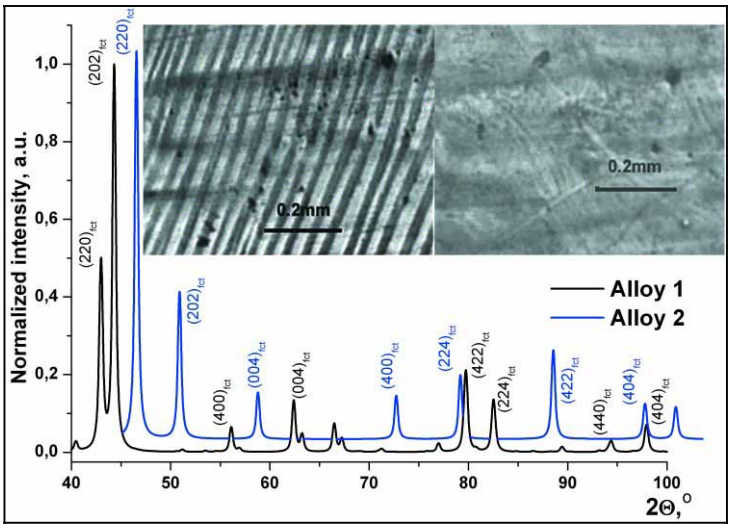

Fig.1. The X-ray powder diffraction patterns collected at CuKα for the martensite crystal lattice determination. Indexing is given within *fct* approximation, according to the parent austenite phase, thus superstuctural peaks are not listed. The insert shows microstructure relief of the Alloy 1 martensite: left – initial twinned, right – detwinned after 1st loading cycle.

All results of experiments conducted in this study are given in Figs.2-4 in engineering stress-strain coordinates, as this system shows directly the true linear elastic deformation dependence on the applied force, as it might be important for possible technical application.

Alloy 1 has a thermoelastic martensite with self-accommodation twinning system [15] with very low critical slip stress (CSS). Thus, as shown on Fig.2, the stress-strain behaviour in the $[100]_{fct}$ direction has a "plastic" character on the 1st cycle, the specimen was originally oriented with the $[100]_{fct}$ axis along the stress direction. However, a stress as low as 0.8MPa leads to detwinning of the martensite and a reorientation of the $[001]_{fct}$ axis in the stress direction. Further cycling, newly along the $[001]_{fct}$ axis (being the axis of easy magnetization of the

martensite) results in elastic deformation, which stabilizes after the 3rd cycle, though some residual twin remains, leading to a non-linear σ(ε) dependence. On the other hand, stress-strain cycling in the $[010]_{fct}$ direction, being also the hard axis of magnetisation (insert on Fig.2), has a pure linear character during the loading stage, the strain is 100% reversible at room temperature and the cycling is stable reaching 4% elastic strain. The martensite $[010]_{fct}$ axis is conserved non-twinned [15], which is also the axis of hard magnetization of the martensite. Unfortunately, the 10M-type Ni-Mn-Ga alloys family, to which belongs the studied Alloy 1, is known to be rather brittle and the specimen fails early during the continuous loading cycles.

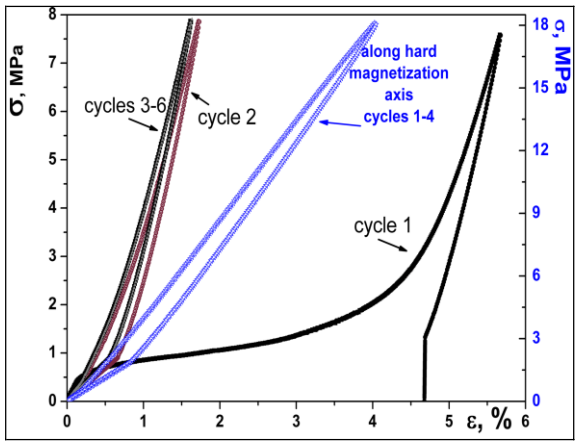

Fig.2. Stress-strain cycling loops of alloy 1 single crystal. Applied stress causes martensite twin variant reorientation, resulting in change of crystallographic direction from [100] in the 1st cycle to [001] in the latter: ε = 1.6% elastic strain obtained. The blue curve shows stress-strain cycling loops of alloy 1 single crystal measured along the "hard magnetization" direction [010]. Strain rate – 1 mm/min ($R = 1.15*10^{-4}$ s^{-1}), at T=295K.

In alloy 2 single crystal, we observe (Fig.3) twin variant reorientation under the applied stress during the first loading cycle, in the same manner as on Fig.2 for alloy 1. However, the CSS in alloy 2 (~14MPa) is more then order of magnitude higher than in alloy 1 (0.6 MPa). Starting with the second cycle, we obtain a 100% reversible superelastic deformation strain of 15.4% at room temperature. Further cycling demonstrates absolute stability and repeatability of the superelastic stress-strain loop (cycles 1-10 of total 50 performed cycles are shown, since later cycling loops looks identical).

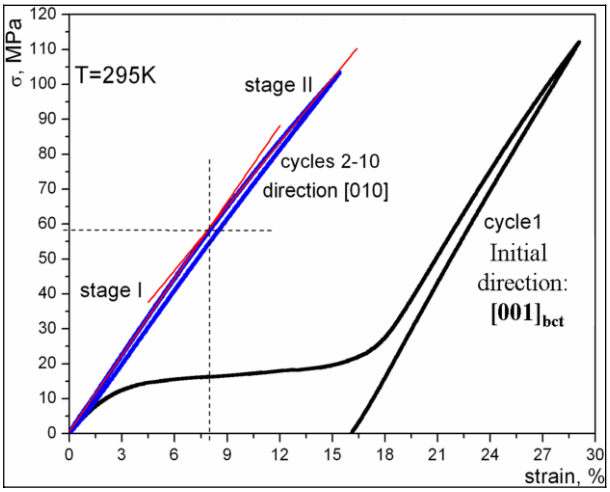

Fig.3. Alloy 2 single crystal elastic stress-strain cycling: absolutely elastic ε = 15.4% strain achieved at the 2nd cycle. Strain rate: 1 mm/min ($R = 1*10^{-4}$ s^{-1}), T=295K.

Closer analysis of the loading phase on alloy 2 reveals that it could be approximated with high confidence ($r > 0.998$) by two linear parts – 1st from 0% to about an 8% deformation, and 2nd – from 8% till the end of the cycle. Stage I seem to correspond to the *eigen*-elastic deformation, while stage II is believed to be due to a stress induced nucleation and growth of another metastable elastic accommodative hierarchical twinning of martensite, incorporating micro- and nano- scales, which decapsulates with stress removal. Such possibility is considered based on the results obtained by V. L'vov and V. Chernenko in [16], that axe-symmetric compression induces the xy-twinned structure of martensite. The critical stress is found to be about 60 MPa at an 8% deformation. The

observed behavior is somewhat analogous to the TiPdNi superelasticity presented in [4], though with a cardinal difference: in our case we observe the superelastic behavior completely in the martensite phase. The unloading stage is linear over the whole range, unlike in [4]. Again, the best superelastic behavior is attributed to the hard magnetization direction. Thus, we can emphasize the clear correlation with the magnetic anisotropy of the martensite, namely the axis of hard magnetization, exhibiting a giant linear rubber-like behavior.

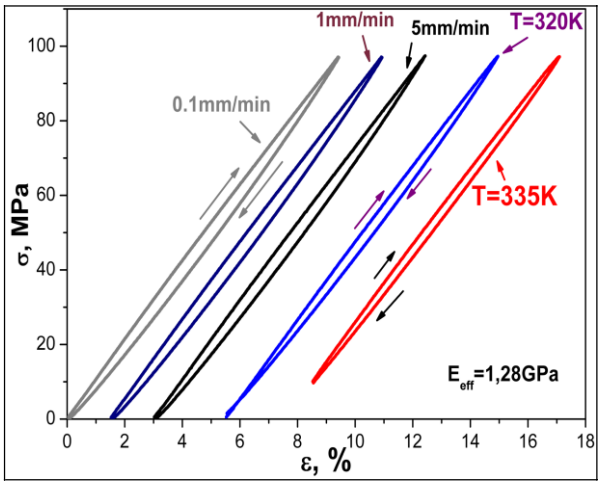

Fig.4. Alloy 2 single crystal elastic loop stability vs loading speed (0.1 mm/min to 5 mm/min, or R = $1*10^{-4}$ to $8.3*10^{-3}$ s^{-1}) and temperature (T = 295K, 320K and 335K). The consequent loops are shifted horizontally for the sake of clarity, in order to avoid overlaps.

Fig.4 presents the stress-strain elastic loops measured with different strain rates – from as slow as 0.1 mm/min up to 5 mm/min (R ~ $1*10^{-4}$ up to $8.3*10^{-3}$ s^{-1}). At constant (room) temperature loops are identical, revealing an absolute stability with respect to the deformation speed in the mentioned range, at variance from the pseudoelasticity reported in SMA, due to stress induced phase transformation. Another crucial point for the possible technical applications is the temperature stability of the effect, evidenced on Fig.4, comparing the series of stress-strain loop measurements at elevated temperatures (T=320K and 335K), compared with those made at T=295K. It can be clearly seen that the elastic behaviour (for alloy 2) is stable with temperature in the martensite phase, at least below T_C, except for the slight slope decrease due to the elastic modulus temperature dependence [17], according to the temperature dependence of the crystal lattice parameters of the martensite.

However, at present, it is not yet clear what the mechanism of a giant martensitic elasticity is. Further work is required to clarify the structural mechanisms and stability of the discussed phenomena. These studies have already started, utilising the in-situ studies with optical microscopy, X-ray and neutron diffraction under stress application, supported with Landau-based modelling approach, and will be submitted for publication in the nearest future.

The studied Ni-Mn-Ga compositions, alloy 2 (with tetragonal non-modulated martensite lattice) looks the most promising for possible technical applications, since it is much more ductile than others [18], making it capable of withstanding many cycles, and has high martensite transformation temperatures – i.e. wide temperature interval for actuation.

4. Conclusions

The phenomenon of giant linear completely elastic deformation (>15%) in the martensite phase of Ni-Mn-Ga at ambient temperature was established.

The superelasticity effect is insensitive to the temperature deviation in the range 295K - 335K. The effect is not sensitive to the loading speed within the interval of 0.1 to 5 mm/min (R ~ $1*10^{-4}$ to $8.3*10^{-3}$ s^{-1}) and stable with continuous mechanical cycling. Alloys with a non-modulated tetragonal type of martensite lattice possess the highest elastic completely reversible deformations and have the widest principal temperature region.

The work was funded by the partner project P-279 between the European Office of Aerospace Research & Development (EOARD), Science and Technology Centre of Ukraine (STCU) and Institute for Metal Physics of National Academy of Sciences of Ukraine. Authors are thankful to Prof. J.L. Martin (EPFL, Lausanne) for the help in the manuscript preparation, and to Prof. V.A. L'vov (Kiev, Ukraine) for fruitful discussions.

References

[1] P.J. Webster, K.R.A. Ziebeck, S.L. Town, M.S. Peak, Philos. Mag. B. **49**, 295 (1984).
[2] V.V. Kokorin, V.V. Martynov, V.A. Chernenko, Scr. Metall. Mater. **26**, 175 (1992).
[3] V.A. Chernenko, V. L'vov, J. Pons, E. Cesari, J. Appl. Phys. **93**, 2394 (2003).
[4] Y. Sutou, N. Kamiya, T. Omori, R. Kainuma, K. Ishida, K. Oikawa, Appl. Phys. Lett. **84**, 1275 (2004).
[5] J. Wua, Q. Tian, Intermetallics **11**, 773 (2003).
[6] Y.F. Zheng, B.M. Huang, J.X. Zhang, L.C. Zhao, Mater. Sci. Eng., A **279**, 25 (2000).
[7] I. Schmidt, R. Lammering, Mater. Sci. Eng., A **378**, 70 (2004).
[8] S. Kajiwara, W.S. Owen, Metall. Trans. **5**, 2047 (1974).
[9] H. Kato, T. Ozu, S. Hashimoto, S. Miura, Mater. Sci. Eng., A **264**, 245 (1999).
[10] F.J. Gil, J.M. Guilemany, Intermetallics **7**, 699 (1999).
[11] L. Anand, M.E. Gurtin, J. Mech. Phys. Solids **51**, 1015 (2003).
[12] D. Entemeyer, E. Patoor, A. Eberhardt, M. Berveiller, Int. J. Plast. **16**, 1269 (2000).
[13] L. Orgeas, A. Vivet, D. Favier, C. Lexcellent, Y. Liu, Scr. Mater. **51**, 297 (2004).
[14] H.B. Xu, Y. Ma, C. Jiang, Appl. Phys. Lett. **82**, 3206 (2003).
[15] G. Mogylnyy, I. Glavatskyy, N. Glavatska, O. Söderberg, Y. Ge, V.K. Lindroos, Scr. Mater. **48**, 1427 (2003).
[16] V.A. Chernenko, V. L'vov, J. Pons, E. Cesari, J. Appl. Phys. **93,** 2394 (2003).
[17] V.A. Chernenko, J. Pons, C. Seguı, E. Cesari, Acta Mater. **50**, 53 (2002).
[18] O. Söderberg, Y. Ge, A. Sozinov, S.-P. Hannula, V.K. Lindroos , Smart. Mater. Struct. **14**, 223–235 (2005)**.**